Journal of Power Sources 196 (2011) 3750–3756

Contents lists available at ScienceDirect

Journal of Power Sources

journal homepage: www.elsevier.com/locate/jpowsour

Prediction and analysis of the cathode catalyst layer performance of proton exchange membrane fuel cells using artificial neural network and statistical methods

N. Khajeh-Hosseini-Dalasm[a,*,1], S. Ahadian[a,b,1], K. Fushinobu[a], K. Okazaki[a], Y. Kawazoe[b]

[a] Department of Mechanical and Control Engineering, Tokyo Institute of Technology, 2-12-1-i6-23, O-okayama, Meguro-ku, Tokyo 152-8552, Japan
[b] Institute for Materials Research (IMR), Tohoku University, Sendai 980-8577, Japan

ARTICLE INFO

Article history:
Received 22 September 2010
Received in revised form
24 November 2010
Accepted 16 December 2010
Available online 24 December 2010

Keywords:
Artificial neural network
Proton exchange membrane fuel cell
Catalyst layer
Agglomerate model
Analysis of means
Analysis of variance

ABSTRACT

A mathematical model was developed to investigate the cathode catalyst layer (CL) performance of a proton exchange membrane fuel cell (PEMFC). A numerous parameters influencing the cathode CL performance are implemented into the CL agglomerate model, namely, saturation and eight structural parameters, i.e., ionomer film thickness covering the agglomerate, agglomerate radius, platinum and carbon loading, membrane content, gas diffusion layer penetration content and CL thickness. For the first time, an artificial neural network (ANN) approach along with statistical methods were employed for modeling, prediction, and analysis of the CL performance, which is denoted by activation overpotential. The ANN was constructed to build the relationship between the named parameters and activation overpotential. Statistical analysis, namely, analysis of means (ANOM) and analysis of variance (ANOVA) were done on the data obtained by the trained neural network and resulted in the sensitivity factors of structural parameters and their mutual combinations as well as the best performance.

1. Introduction

One of the main obstacles for the mass production of proton exchange membrane fuel cell (PEMFC) is its cost and durability balance. It is significantly affected by catalyst layer (CL) design and performance especially cathode catalyst layer. The key electrochemical reaction takes place in the cathode CL in which oxygen molecule is combined with proton H^+ and generates electrical current. The amount of generated current as a result of electrochemical reaction depends on the CL structural parameters and also the way the CL is synthesized. A robust and reliable PEM fuel cell performance analysis requires a thorough understanding of CL performance through extensive parametric studies. Since experimental investigations are very time consuming and costly, numerical simulation can be very useful in CL performance prediction.

In order to reliably predict the CL performance, an agglomerate model is developed to capture the complex multi-material structure of the CL. Agglomerate models seem to predict the CL performance better compared to interface model and macro-homogeneous model [1]. Here, we focus on agglomerate model to investigate the CL performance and we would like to know: (1) Since the solution of numerical model can be complicated and time consuming, is there a general model to describe the CL performance with respect to independent parameters in a simple and easy way? (2) Since many CL parameters especially CL structural parameters are involved in the numerical simulation, how much is the influence of various parameters affecting the CL performance? To address the above questions, an artificial neural network (ANN) approach is employed.

There are several studies about the ANN modeling of fuel cells parameters based on simulated and experimental data. Lee et al. [2] have used a feed forward back propagation network in which the cell potential was modeled as a function of four input variables (i.e., current density, reactant pressures and cell temperature) based on experimental data set. It was shown that the ANN can predict well the fuel cell power system. Wu et al. [3] have applied the ANN to simulate an experimental data set with six input independent variables (i.e., operating temperature and pressure, anode and cathode humidification temperature, anode and cathode stoichiometric flow ratio) with respect to electrical power. The performance of three different types of ANN, namely, multi layer perceptron, generalized feed forward network, and Jordan and Elman network has been examined and compared by Lobato

* Corresponding author. Tel.: +81 3 5734 2179; fax: +81 3 5734 2179.
E-mail address: khajehhosseini.n.aa@m.titech.ac.jp
(N. Khajeh-Hosseini-Dalasm).
[1] Authors who equally contributed to the paper.

0378-7753/$ – see front matter © 2010 Elsevier B.V. All rights reserved.
doi:10.1016/j.jpowsour.2010.12.061

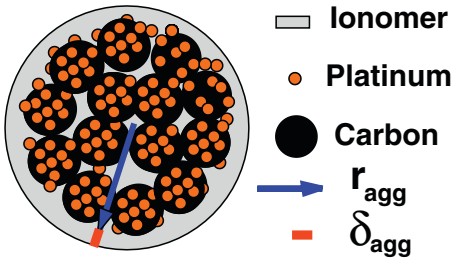

Fig. 1. Schematic representation of an agglomerate structure for catalyst layer (CL).

et al. [4]. These three types were used to model the performance of a polybenzimidazole–polymer electrolyte membrane fuel cell in which the designed network had three input variables (conditioning and operating and current density) and three output variables (potential, cathode and ohmic resistance). A high power PEM fuel cell model was simulated employing ANN using the data set obtained by a dynamic model and experiments by Sisworahardjo et al. [7]. They have found a close agreement between the outputs of the designed ANN and the experimental results.

To the best of authors' knowledge, there is no previous report of the application of ANN approach on CL modeling. In this paper, a methodology based on ANN was applied to study the dependence of CL performance on the CL structural parameters. An spherical agglomerate structure for the CL is considered, which takes into account the effects of the liquid water saturation and eight structural parameters (i.e. ionomer film thickness covering the agglomerates, agglomerate radius, platinum and carbon mass loading, gas diffusion layer (GDL) penetration fraction and porosity, and CL thickness). First, some input and corresponding output data points obtained from the developed agglomerate CL model were used to train the ANN. The designed ANN was then employed to predict the performance of the CL for unseen input data points. In addition, statistical methods were employed to identify the effect of each input parameter as well as their combinations on the CL performance (determined by activation overpotential). Interesting results were attained and discussed.

2. Model description

Here, a one dimensional steady state mathematical model for the cathode CL based on a homogenous agglomerate structure is developed. Fig. 1 represents a schematic representation of an agglomerate structure for CL. It is assumed that the CL is constituted of partially flooded spherical agglomerates with the average radius of r_{agg}. Each agglomerate consists of platinum and carbon (Pt/C) particles that are bonded together with fully saturated electrolyte (ionomer phase) and GDL material. Agglomerate may be covered by an evenly distributed ionomer with the thickness of δ_{agg}. The transport of oxygen within the porous cathode CL is governed by Fick's law of diffusion as follows [5]

$$\frac{dC_{O_2}}{dz} = \frac{i - I}{4FD^{eff}_{O_2}} \tag{1}$$

The electrochemical reaction rate for the agglomerate covered with ionomer having the thickness of δ_{agg} is obtained from [6]

$$\frac{di}{dz} = 4F\left(\frac{1}{Ek_1A} + \frac{\delta_{agg}}{a_{agg}D_{O_2,m}}\frac{r_{agg}+\delta_{agg}}{r_{agg}}\right)^{-1}\frac{C_{O_2}}{K_{O_2}} \tag{2}$$

where the first order reaction rate constant k_1 is related to activation overpotential η and exchange current density i_0 via Tafel

Table 1
Constitutive relations.

Parameters	Expressions
$D^{eff}_{O_2}$	$D^{eff}_{O_2-g}\frac{(1-s)\varepsilon_c}{\varepsilon_c+L_s} + D^{eff}_{O_2-w}\frac{s\varepsilon_c}{\varepsilon_c+L_s}$
$D^{eff}_{O_2-g}$	$\left(\frac{1}{(\varepsilon_c(1-s))^{3/2}}\left(\frac{1}{D_{O_2-g}} + \frac{1}{D_{Kn}}\right)\right)^{-1}$
$D^{eff}_{O_2-w}$	$(\varepsilon_c s)^{3/2} D_{O_2-w}$
E	$\frac{1}{M_T}\left(\frac{1}{tangh(3M_T)} - \frac{1}{3M_T}\right)$
M_T	$\frac{r_{agg}}{3}\sqrt{\frac{k_1 a}{D^{eff}_{O_2-g}}}$
K_{O_2}	$\frac{1}{RT}\exp\left(-\frac{666}{T} + 14.1\right)$
κ^{eff}	$(1-\varepsilon_c)\left(1 + \frac{\varepsilon_{agg}-1}{(1+\delta/r_{agg})^3}\right)\kappa$
σ^{eff}	$(1-\varepsilon_c)^{3/2}\sigma$
ε_c	$1 - \frac{1}{l_c}\left(\frac{m_{Pt}}{\rho_{Pt}} + \frac{m_C}{\rho_C}\right) - L_{m,c} - L_s$
L_s	$L_{g,c}(1-\varepsilon_g)$
ε_{agg}	$\frac{L_{m,c}+n_{agg}\frac{4}{3}\pi r^3_{agg}}{(1-\varepsilon_c)} - 1$
A_s	$(227.79f^3 - 158.57f^2 - 201.53f + 159.5)\times 10^3$
A	$\frac{m_{Pt}}{l_c}A_s$
a	$\frac{A}{n_{agg}\frac{4}{3}\pi r^3_{agg}}$
a_{agg}	$4\pi r^2_{agg} n_{agg}$
n_{agg}	$\left[\frac{4}{3}\pi\left(r_{agg}+\delta_{agg}\right)^3\right]^{-1}(1-\varepsilon_c)$
d_{avg}	$\frac{4}{3}\frac{\varepsilon_c}{1-\varepsilon_c}r_{agg}$
D_{Kn}	$\frac{1}{3}d_{avg}\sqrt{\frac{8RT}{\pi M_{O_2}}}$

expression

$$k_1 = \frac{1}{4F}\frac{i_{0,ref}}{C^{ref}_{O_2}}\left[\exp\left(\frac{\alpha_c F}{RT}\eta\right) - \exp\left(-\frac{\alpha_a F}{RT}\eta\right)\right] \tag{3}$$

Finally, an expression for the activation overpotential can be obtained using Ohm's law [5]. There is a resistance against the proton and electron migration through the polymer and solid portions of the CL, respectively. Therefore,

$$\frac{d\eta}{dz} = \frac{i}{\kappa^{eff}} + \frac{i-I}{\sigma^{eff}}. \tag{4}$$

Eqs. (1), (2), and (4) comprise a coupled nonlinear ODEs with the unknowns C_{O_2}, i, and η that govern the oxygen, proton and electron transport within the agglomerates. Boundary conditions are needed to solve the ODEs and are given in detail in Ref. [8]. As it was shown, the GDL/CL interface corresponds to $z = 0$ and the CL/membrane interface corresponds to $z = l_c$. Other necessary relationships and constitutive equations are listed in Table 1. Other necessary constants in Table 1, i.e., κ and σ can be found in the previous study of the author [8].

3. Design of artificial neural network

An ANN is a calculation processing paradigm that has been inspired by the way biological neurons and brain process the information. The key element of a biological neural system is the parallel distributed process nature. It composes of a great number of highly interconnected simple process units called neuron working in a unit union. This is true of ANNs as well. A typical ANN is shown in Fig. 2. It is seen that an ANN consists of a network with three main elements, i.e., input vector, hidden layer(s), and output layer. As illustrated in Fig. 3, each neuron receives an input P. Each input is multiplied by an associated weight W and then is added by a bias b. The product $(WP + b)$ is the net input shown by n. The net input

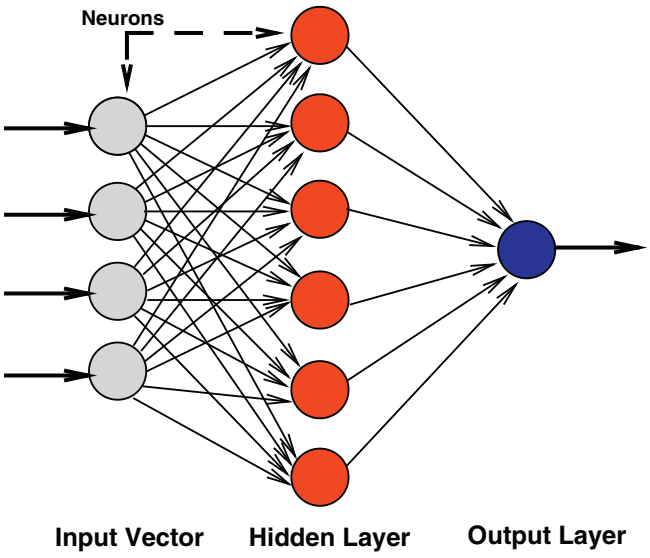

Fig. 2. Schematic diagram of a typical artificial neural network (ANN).

is an argument of a transfer function f, which determines a neuron output a. A typical transfer function f is log-sigmoid, which is also used in this study and has the following form

$$a = f(WP + b) = \frac{1}{1 + \exp(-(WP + b))} \quad (5)$$

This transfer function takes any value and squashes the output a between 0 and 1. The neuron shown in Fig. 3 is a simplified neuron model firstly introduced by McCulloch and Pitts [9]. They showed the network of these artificial neurons can compute any arithmetic or logical function. The greatest advantage of ANNs could be their ability to serve as an approximation model for any arbitrary function [10].

In this study, an ANN system for the prediction of cathode CL performance of a PEMFC determined by its activation overpotential was put to test. Here, we used the numerically attained data set by the mathematical model in which the activation overpotential can be computed as a function of saturation and eight CL structural parameters, i.e., ionomer film covering the agglomerate, agglomerate radius, platinum and carbon loading, membrane content, GDL penetration content, and CL thickness. Each input parameter for the present study changes in three levels as shown in Table 2. It is noted that a cell current density of $I = 5000\ \mathrm{A\ m^{-2}}$ is considered.

After preparing the data set, an ANN is designed to find the relationship between the dependent parameter (i.e., activation overpotential) and the input parameters (i.e., saturation, ionomer film covering the agglomerate, agglomerate radius, platinum and carbon loading, membrane content, GDL penetration content, and CL thickness). Here, a back propagation feed forward network with one hidden layer and Levenberg–Marquardt learning algorithm is employed. A detailed description of back propagation algorithm can be found in Ref. [11]. A back propagation trained neural network is constructed by selecting an appropriate architecture of neurons in the network. This includes how many layers of the neurons should be used, the number of neurons in each layer, and how neurons

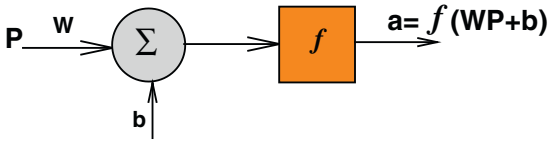

Fig. 3. Mathematical model of a neuron.

Table 2
Input parameters and their corresponding values used in this work.

Independent variables	Level 1	Level 2	Level 3
s	0	0.6	1
δ_{agg}	0	40×10^{-9}	80×10^{-9}
r_{agg}	0.25×10^{-6}	0.5×10^{-6}	1×10^{-6}
m_{Pt}	0.04	0.05	0.06
m_C	0.002	0.003	0.004
$L_{m,c}$	0.1	0.25	0.4
$L_{g,c}$	0.05	0.1	0.15
ε_g	0.3	0.4	0.45
l_c	1×10^{-5}	3×10^{-5}	5×10^{-5}

should be connected. In the present study, a network architecture with one hidden layer is selected, which was shown to capture any complex relationship that may exist between the input(s) and output(s) [12]. The number of neurons is selected to give the best performance for the designed ANN.

After the network architecture has been designed, the network is trained. Training is done by assigning random weights and biases to each neuron, presenting a series of input and output values as a training data set and evaluating the error. In the training procedure, the network's unknowns, i.e., weights and biases are determined to reduce the difference between the predicted output and the actual value. The training process continues until the network ability to generalize, as measured by its predictive performance on the test data set, is optimal. 10 percent of the whole data set is kept for testing data. It means that 90 percent of the available data set was used for training. The performance of the ANN is evaluated by the squared correlation coefficient (R^2) and mean square error (MSE), which show the accuracy of the target output toward the predicted output by the trained ANN [13]. It is noted that for a perfect correlation R^2 and MSE should be 1 and 0, respectively. The best neural network design was found to have one hidden layer with 18 neurons. Fig. 4 presents the training process of the designed ANN with the training cycle (i.e., epoch). As can be seen, the MSE monotonically declines for training data set with epochs. Finally, it reaches a value smaller than 0.002 after 2000 epochs. The corresponding R^2 and MSE were 0.8 and 0.0016, respectively, for the test data set. Fig. 5 displays the comparison of activation overpotential of numerical data points with the ones predicted by the designed ANN. It can be observed a good agreement between the numerical data and the predicted data. Therefore, our proposed ANN is able to model and predict the CL performance with respect to the input parameters.

One can say that it is feasible to fit the activation overpotential as a function of underlying independent parameters using a

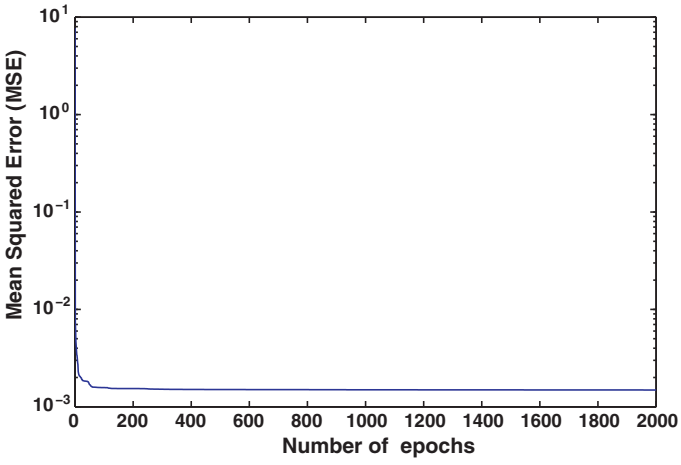

Fig. 4. Plot of the mean squared error (MSE) versus the number of epochs for training of the designed artificial neural network (ANN).

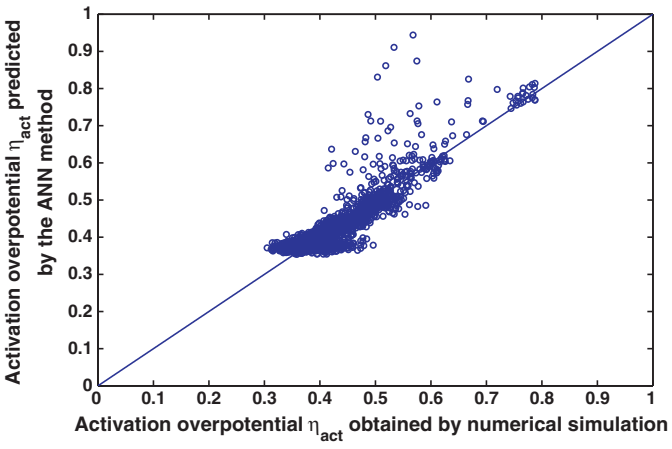

Fig. 5. Plot of the activation overpotential predicted by ANN method versus the corresponding activation overpotential obtained by the numerical simulation for the test data set.

polynomial function. Therefore, we should mention some advantages of the ANN method over the polynomial fitting as listed below.

- The ANN method can globally search a highly dimensional space of independent parameters in a rapid and easy way. However, in contrast to the ANN method, the polynomial fitting needs a tedious and time-consuming procedure to do such a global searching. Therefore, one can essentially achieve more accurate and reliable results in a specified computational time using the ANN method compared to those obtained by the polynomial fitting.
- The ANN method is quite flexible to estimate an arbitrary objective function (here, the activation overpotential) as compared to the polynomial fitting since there are a lot of options to design an ANN such as the type of activation functions, the number of layers, the number of neurons per hidden layer(s) and so on.
- The results modeled or predicted using the ANN method are easily tractable since they can be directly analyzed with the available statistical tools. A good example has been illustrated in this case study.

4. Results and discussion

The designed ANN model could be applied to make further prediction of CL performance for data points, which not belong to the numerical data set.

Two preliminary advantages of ANN are its massively parallel-distributed structure and its ability to learn and therefore generalize. The first advantage, i.e., massive parallel-distributed structure gives this ability to ANN to process the information with high speed. The second advantage, i.e., generalization refers the ability of ANN to produce reasonable output(s) for input(s) not encountered during the training process [14]. A well-designed ANN is able to generalize providing its performance against the test data set is very good. Generally speaking, the central idea of using ANN is to perfectly predict the results, i.e., output for a set of input parameters for the unseen data set without necessarily expending much time and energy on numerical simulation and/or experiment. The time consumed for the numerical simulations for 19,683 data points was about 10 h on a CPU with a clock speed of 1.4 GHz. While, the time needed for the designed ANNs to provide the rest of data set (72,900 data points) was about 5 min on the same CPU. Moreover, the prediction process using the ANN method does require little or no human intervention compared to that of the numerical calculations. Additionally, an ANN ignores large noises or variations while it drives principle rules for a given problem. Generally, such noises and variations can be expected in numerical simulations and experiments.

Despite the aforementioned interesting characteristics, ANNs provide no information of physical interpretations concerning underlying problems. ANNs are generally perceived as being a black box and are not able to give explanation of how outputs are obtained. However, it is desirable to extract knowledge from the trained ANNs so that one can gain a better understanding of the solution. To this end, two statistical methods, namely, analysis of means (ANOM) and analysis of variance (ANOVA) were employed. It is emphasized that the complete data set obtained with the aid of the ANN approach is required to statistically analyze the CL performance (determined by activation overpotential).

Both ANOM and ANOVA are based on the principle of linear superposition approximation [15]. The ANOM is used to determine the main effect of each independent input variable on the dependent output variable, i.e., activation overpotential. The ANOM value for each level of a parameter is determined while all other parameters' levels are varied. The ANOM plot shows the average trend of the output parameter versus each input independent variable. While ANOM does not determine the possible interactions between the input parameters, ANOVA can be performed for the consideration. The interaction term implies how the combined independent variables affect the target output. Furthermore, in the present study, ANOVA is used to quantify the importance of the parameters, which can affect the CL performance. The mathematical treatment of these statistical methods, i.e., ANOM and ANOVA has been given in our previous work [16].

The results of the ANOM procedure concerning the effect of input parameters (i.e., saturation, Nafion film covering the agglomerate, agglomerate radius, platinum and carbon loading, membrane content, GDL penetration content, and CL thickness) on the output (i.e., activation overpotential) are demonstrated in Fig. 6 and discussed below.

1. Liquid water saturation 1 corresponds to fully flooded CL and 0 liquid water saturation corresponds to fully open pores of CL. It has been observed (Fig. 6-(1)) that the CL performance deteriorates when the liquid water saturation increases. The reason is that there is a direct relationship between the diffusion resistance of oxygen to reach the reaction site and the liquid water saturation due to less open pore spaces. It is worthwhile to mention that in the case of fully flooded pores, the effective oxygen diffusion coefficient is in the order of 10^{-9} and in the case of no liquid water, it has the order of 10^{-6}.
2. As can be seen in Fig. 6-(2), there is a slight increase of activation overpotential from zero to 0.4×10^{-7} followed by steeper increase. An increase in the thickness of ionomer film covering the agglomerates causes a decrease in the reaction rate resulted from higher resistance against the oxygen diffusion into the agglomerate. The optimum value is acquired at the zero ionomer thickness. This agrees with the numerical optimization of Secandell et al. [17] where it was concluded that adding the ionomer film has no benefit.
3. Increasing agglomerate radius has two competing effects (see Fig. 6-(3)). Higher radius of agglomerates increases the diffusion length of dissolved oxygen inside the agglomerate as a results of longer diffusion length. On the other hand, it leads to bigger pores between the agglomerates and therefore higher diffusion coefficient of oxygen. It can be seen that the ANN prediction in Fig. 6-(3) proposes an optimum value for the agglomerate radius

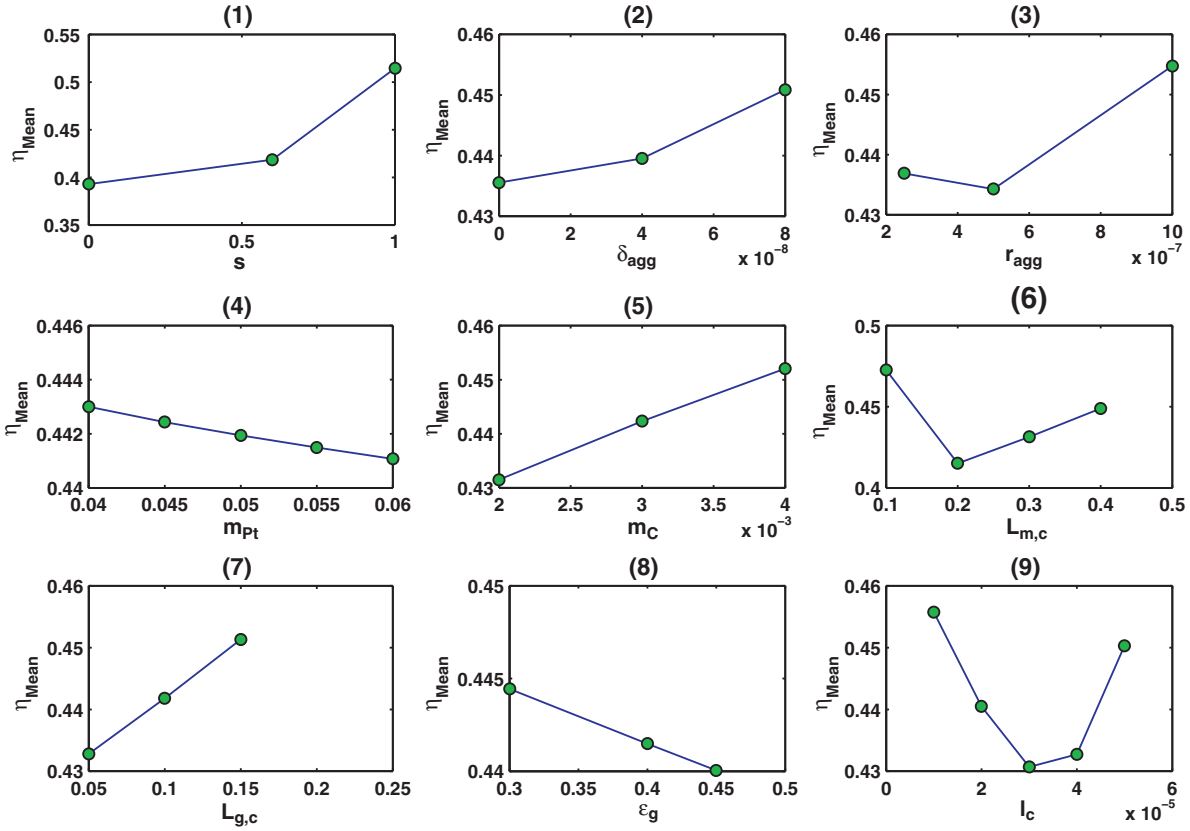

Fig. 6. Main effects of the input parameters (i.e., saturation and eight structural parameters, i.e., ionomer film thickness covering the agglomerate, agglomerate radius, platinum and carbon loading, membrane content, gas diffusion layer penetration content and CL thickness) on the CL activation overpotential obtained by the analysis of means (ANOM).

r_{agg}. The optimum value for r_{agg} has been also observed in the numerical study of Kamarajugadda et al. [18].

4. Increasing platinum mass loading has two competing effects as shown in Fig. 6-(4). First, it increases the accessible reaction surface area, which tends to decrease the activation overpotential. Second, it may result in lower porosity and therefore lower oxygen diffusion coefficient. This tends to increase the activation overpotential. These two effects therefore compete with each other with the net result being that activation overpotential decreases with m_{Pt}. This predicted result by ANN agrees with the numerical simulation of Sun et al. [6].
5. The main effect of increasing carbon mass loading is to reduce porosity and consequently lower oxygen diffusion coefficient. This leads to higher activation overpotential (see Fig. 6-(5)).
6. Increasing ionomer loading has two competing effects. First, as porosity decreases, the resistance to oxygen diffusion increases. Second, as ionomer content inside the agglomerate increases, the activation overpotential decreases. These two effects therefore compete with each other with the net result being demonstrated in Fig. 6-(6). The observed trend is in agreement with the experimental results reported by Song et al. [19] and the numerical predictions by Yin [20].
7. The average changes of activation overpotential in response to changes in GDL penetration portion in the CL is displayed in Fig. 6-(7). Since this parameter limits the CL porosity by its penetration, the CL activation overpotential increases.
8. Fig. 6-(8) shows the average changes of activation overpotential with respect to changes in GDL porosity. In fact, the CL porosity increases as we increase the amount of pores in GDL. Therefore, the CL performance is enhanced and activation overpotential decreases.
9. The behavior of the activation potential with respect to the CL thickness has two opposing effects as we increase the CL thickness. First, it should be increased since the oxygen diffusion length increases. Second, the amount of porosity also increases and it enhances the CL performance. The final outcome is demonstrated in Fig. 6-(9). The existence of a minimum activation overpotential (i.e., optimum performance) with respect to the CL thickness has been also observed in previous studies [18,21].

We note that the optimum performance is achieved at some intermediate points for agglomerate radius r_{agg}, membrane content $L_{m,c}$, and catalyst thickness l_c and one of the endpoints of the range for other parameters.

In order to attain a more accurate indication of the relative importance of the independent variables and their interactions, ANOVA test was used. The obtained ANOVA table in this study is summarized in Table 3. Let us look at the calculated F values for each parameter, which has been shown in the column 5 of Table 3. The F value for each parameter is simply the ratio of the mean square deviation of that parameter to the mean square error. This statistic is used to determine the significance of input parameters, which include CL structural characteristics. In general, a value of F less than 1 implies that the effect of the corresponding given input parameter is smaller than the error associated with the linear superposition approximation and therefore can be ignored. On the other hand, a value of F above 4 generally suggests that the effect of the independent variable is quite significant. As can be observed, s, $L_{m,c}$, and l_c have the largest influence on the CL activation overpotential η. The effect of $L_{g,c}$, m_c, r_{agg}, and δ_{agg} was also significant but not as much as the effect of s, $L_{m,c}$, and l_c. The effect of the other parameters, i.e., m_{Pt}, ε_g is insignificant. The interaction effect between

Table 3
The analysis of variance (ANOVA).

Source	Degree of freedom	Sum of squares	Mean square	F
s	2	87.183	43.591	12,500
δ_{agg}	2	0.70545	0.35275	100.75
r_{agg}	2	3.597	1.7984	513.79
m_{Pt}	4	0.07365	0.0184	5.26
m_C	2	3.0856	1.5428	440.75
$L_{m,c}$	3	9.8576	3.2859	938.81
$L_{g,c}$	2	1.6184	0.8092	231.17
ε_g	2	0.101	0.05055	14.44
l_c	4	3.0864	0.7716	220.66
$\delta_{agg} \times r_{agg}$	4	0.1696	0.0424	12.115
$m_{Pt} \times m_C$	8	0.0796	0.00995	2.845
$L_{m,c} \times L_{g,c}$	6	0.52105	0.08685	24.785
Error	36,408	127.46	0.0035	
Total	36,449	237.63		

the agglomerate's geometry parameters ($\delta_{agg} \times r_{agg}$) on the CL performance is more significant than those interaction parameters of catalyst particles mass loading ($m_{Pt} \times m_C$) and membrane-GDL content ($L_{m,c} \times L_{g,c}$).

Note that the value of the activation overpotential at a specified level of an independent parameter is the average value of all activation overpotentials while all other independent variables change within their acceptable ranges. Therefore, the activation overpotential values for a given independent parameter are not essentially the same and therefore are subject to the statistical errors. As can be observed, the significance of each independent parameter has been measured in terms of F statistic for each independent variable in Table 3. In addition, as you noticed, the computed F values would be different if one changes the range of independent parameters. However, notice that the selected range of each independent parameter is acceptable and can be used (or observed) in some practical circumstances. Therefore, it would be useful to compare the significance of underlying independent parameters, which can be changed within the range defined in this work.

5. Conclusion

For the first time, a novel methodology, namely, ANN approach together with statistical methods (ANOM and ANOVA methods) were employed for modeling, prediction, and analysis of an agglomerate cathode CL performance. It was shown that the designed ANN is capable of modeling and predicting the cathode CL activation overpotential for different input parameters including eight structural parameters. Instead of solving the ODEs, the ANN provides a simple and direct means for the prediction of activation overpotential and is able to consider the effect of influencing parameters simultaneously. ANOM and ANOVA methods also allowed us extract physical explanations regarding the underlying system modeled using the ANN approach. Cathode CL thickness and the membrane volume content in CL were found to be the most significant structural parameters affecting the CL performance.

List of symbols

a	active surface area within the agglomerate (m^{-1})
a_{agg}	total external area of active sites of agglomerate per unit volume of CL (m^{-1})
A	total active area of agglomerate per unit volume of CL (m^{-1})
A_s	reaction surface area per unit mass of platinum ($m^2\ kg^{-1}$)
C	concentration ($mol\ m^{-3}$)
d_{avg}	average pore diameter (m)
D_{O_2}	diffusion coefficient ($m^2\ s^{-1}$)
D_{Kn}	Knudsen diffusion coefficient ($m^2\ s^{-1}$)
f	mass fraction of platinum to that of Pt/C particles
F	Faraday constant (96, 485 coulombs mol^{-1})
i	local current density ($A\ m^{-2}$)
i_0	exchange current density ($A\ m^{-2}$)
I	cell current density ($A\ m^{-2}$)
k_l	reaction rate constant ($m\ s^{-1}$)
l_c	catalyst layer thickness (m)
$L_{g,c}$	volume fraction of GDL penetrating into the CL
$L_{m,c}$	voltage fraction of the ionomer phase in the CL
L_s	volume fraction of the GDL solid material penetrated into the CL
m_{Pt}	platinum mass loading ($kg\ m^{-2}$)
m_C	carbon mass loading ($kg\ m^{-2}$)
M	molecular weight ($kg\ mol^{-1}$)
M_T	Thiele module
n_{agg}	number of agglomerates per unit volume of CL (m^{-3})
P	pressure (Pa)
r_{agg}	agglomerate radius (m)
R	universal gas constant ($8.314\ J\ mol^{-1}\ K^{-1}$)
s	liquid water saturation
T	temperature (K)
V	volume (m^3)
r, z	coordinate (m)

Greek letters

α	transfer coefficient
δ_{agg}	ionomer film thickness (m)
ε_c	CL porosity
ε_g	GDL porosity
η	activation overpotential (V)
ρ_C	carbon density ($kg\ m^{-3}$)
ρ_{Pt}	platinum density ($kg\ m^{-3}$)
σ	electronic conductivity ($S\ m^{-1}$)
κ	protonic conductivity ($S\ m^{-1}$)

Acknowledgments

This work has been partly supported by the ENERGY-GCOE program at Tokyo Institute of Technology and the Grant-in-Aid for Scientific Research from MEXT/JSPS. S. Ahadian appreciates the Japan Society for the Promotion of Science (JSPS) for financial support.

References

[1] J. Xhang, PEM Fuel Cell Electrocatalysts and Catalyst Layers: Fundamentals and Applications, Springer, London, 2008.
[2] W.Y. Lee, G.G. Park, T.H. Yang, Y.G. Yoon, C.S. Kim, Int. J. Hydrogen Energy 29 (2004) 961–966.
[3] S.J. Wu, S.W. Shiah, W.L. Yu, Renew. Energy 34 (2009) 134–144.
[4] J. Lobato, P. Canizares, M.A. Rodrigo, J.J. Linares, C.G. Piuleac, S. Curteanu, J. Power Sources 192 (2009) 190–192.
[5] C. Marr, X. Li, J. Power Sources 77 (1999) 17–27.
[6] W. Sun, B.A. Peppley, K. Karan, Electrochim. Acta 50 (2005) 3359–3374.
[7] N.S. Siswarahardjo, T. Yalcinoz, M.Y. El-Sharkh, M.S. Alam, Int. J. Hydrogen Energy 35 (2010) 9104–9109.
[8] N. Khajeh-Hosseini-Dalasm, M.J. Kermani, D. Ghadiri Moghaddam, J.M. Stockie, Int. J. Hydrogen Energy 35 (2010) 2417–2427.
[9] W. McCulloch, W. Pitts, Bull. Math. Biophys. 5 (1943) 115–133.
[10] T. Hastie, R. Tibishrani, J. Freidman, The Elements of Statistical Learning: Data Mining, Inference and Prediction, Springer, New York, 2001.
[11] M.T. Hagan, H.B. Demuth, M. Beale, Neural Network Design, PWS, Boston, 1996.
[12] K. Hornik, M. Stinchcombe, H. White, Neural Networks 2 (1989) 359–366.
[13] N.R. Draper, H. Smith, Applied Regression Analysis, Wiley, NewYork, 1998.
[14] S. Haykin, Neural Networks: A Comprehensive Foundation, Prentice Hall, New Jersey, 1999.

[15] D.C. Montgomery, E.A. Peck, G.G. Vining, Introduction to Linear Regression Analysis, Wiley–Interscience, Hoboken, 2006.
[16] S. Ahadian, H. Mizuseki, Y. Kawazoe, Microfluid. Nanofluid. 9 (2010) 319–328.
[17] M. Secandel, K. Karan, A. Suleman, N. Djilali, Electrochim. Acta 52 (2007) 6318–6337.
[18] S. Kamarajugadda, S. Mazumder, J. Power Sources 183 (2008) 629–642.
[19] J.M. Song, S.Y. Cha, W.M. Lee, J. Power Sources 94 (2001) 78–84.
[20] K.M. Yin, J. Electrochem. Soc. 153 (2005) A583–A593.
[21] D. Song, Q. Wang, Z.S. Liu, C. Huang, J. Power Sources 159 (2006) 928–942.